Microphase Segregation of PEO−PAMAM Linear−Dendritic Diblock Copolymers

Mark A. Johnson, Jyotsna Iyer, and Paula T. Hammond*

Department of Chemical Engineering, Massachusetts Institute of Technology, Room 66-550, 77 Massachusetts Avenue, Cambridge, Massachusetts 02139-4307

Received August 28, 2003

ABSTRACT: Transmission electron microscopy and X-ray scattering have been used to characterize the microphase segregation of linear−dendritic diblock copolymers in the bulk state. The dendritic block copolymers consisted of a linear poly(ethylene oxide) (PEO) block of 2000 molecular weight attached covalently to a polyamidoamine (PAMAM) dendron. The morphology and temperature dependence of diblocks containing dendrons of generations 1.0−4.0 was characterized. In addition, the dendritic end groups were functionalized with stearic acid to make amphiphilic linear−dendritic diblock copolymers. The morphology and temperature dependence of these materials was also characterized. Results indicate that the unfunctionalized diblocks exhibit a segregated melt state above the PEO melting point and that the PEO block undergoes confined crystallization below its melting point. The glass transition of the PAMAM block is below room temperature such that the PEO crystallinity is weakly confined by the PAMAM domains. The stearate functionalized diblocks also exhibit a segregated melt state at high temperature. However, at low temperatures both the stearate and PEO are crystalline and crystallization is strongly confined within lamellar domains.

1. Introduction

Dendritic molecules present a number of new possibilities in the areas of molecular engineering and nanotechnology due to their unique structure and properties. These macromolecular systems undergo systematic branching from a central core, resulting in materials with nanometer scale dimensions, porous or swellable interior regions, and a dense distribution of end functional groups for higher generations at the exterior of the dendrimer. These characteristics have made dendrimers interesting for a number of applications. Small molecules have been bound or encapsulated in the interior regions of dendrimers,[1] leading to the potential use of dendrimers in encapsulation and the controlled release of drugs, as well as metal nanoparticle formation[2−5] for surface catalysis and magnetic storage media. Other applications include selective ion membranes, heavy metal or toxic agent removal, and reactive thin film membranes. In the bulk state, the spherical shape and dense outer shell associated with high generation dendrimers results in few entanglements between molecules (they have been termed molecular ball bearings[6]) and poor cohesive film-forming properties. Diblock copolymers consisting of a linear block attached covalently to a dendrimer or dendron offer an opportunity to introduce greater mechanical stability via the presence of phase segregated morphologies, and the introduction of entanglements in the case of linear blocks with molecular weights sufficiently higher than the entanglement molecular weight. A number of potential applications would benefit from the formation of organized dendritic nanostructures within a continuous supporting matrix, to allow the formation of dendritic materials into thin cohesive films with good mechanical properties, while maintaining the advantage of the unique architecture of dendrimers. A further, and perhaps more important, advantage to the use of block copolymers is the fact that segregation of the dendrimer block can be used to create ordered arrays of dendrimers in the solid state, which allow the development of membranes, microreactors, delivery devices, and other nanostructured materials containing dendritic elements.

While there are numerous reports on the synthesis and characterization of dendritic homopolymers and diblocks, there is still much to understand about the morphology and self-assembly behavior of linear−dendritic diblock systems. The nonsymmetric mass distribution in such systems, and the highly branched nature of the dendrimer, can result in more complex phase behavior; further complex morphologies may be induced by the presence of a crystallizable linear block. Both crystalline and amorphous linear blocks have been explored in the literature. Gitsov, Wooley, and Fréchet were the first to introduce linear−dendritic diblock copolymers by attaching convergently synthesized benzyl ether dendrons to one or both terminal end groups of linear poly(ethylene glycol) (PEO);[7] these block copolymers and related star copolymers illustrated a range of interesting solvent dependent solution behavior.[8,9] In a discussion of the material bulk behavior, it was observed that crystallinity in the PEO block decreases with increasing dendrimer generation in thin films cast from THF and $CHCl_3$.[10] Meijer and co-workers have reported on the synthesis and properties of amphiphilic diblock copolymers of polystyrene and acid-functionalized polypropyleneimine dendrimer[11] that exhibited generation-dependent aggregation in solution and microphase segregation in the solid state. In the bulk state, Meier and co-workers observed a transition from cylindrical to lamellar morphology with increasing dendrimer generation, consistent with a shift in the morphology/volume fraction phase diagram toward more continuous morphologies at relatively low dendrimer volume fractions. Similar observations have recently been made by Mackay et al.[35] and Pochan et al.[36] with poly(benzyl ether) diblock copolymers.

Our research group has also reported the synthesis and properties of linear−dendritic diblocks consisting

10.1021/ma030450m CCC: $27.50
Published on Web 03/06/2004

Table 1. Summary of Molecular Weights and Compositions for PEO−PAMAM and Stearate D_{35}-Functionalized PEO−PAMAM Samples

PAMAM generation	MW	vol fraction[a] PAMAM	wt fraction[b] PAMAM	wt fraction[b] PAMAM + stearate
1	2230	0.03	0.10	
2	2686	0.08	0.26	
3	3619	0.22	0.45	
4	5420	0.42	0.63	
1-S_{D35}	2834	0.03	0.08	0.29
2-S_{D35}	3890	0.06	0.18	0.49
3-S_{D35}	6035	0.13	0.27	0.67
4-S_{D35}	10 252	0.21	0.33	0.80

[a] Volume fraction determined by dividing the volume of the PAMAM dendron by the sum of the dendron volume plus the volume of all the monomer units forming the linear block and any attached stearate groups based on density. PAMAM dendrons are assumed to have a conical unit volume with dimensions consistent with the corresponding spherical dendrimer homopolymer.[16,17] [b] Weight fraction calculated by dividing the MW of the PAMAM block by the total MW of the diblock. Complete formation of all dendron branches and complete conversion of all reactive branch ends during stearate functionalization are assumed.

of a semicrystalline poly(ethylene oxide) (PEO) linear block and polyamidoamine (PAMAM) dendrons.[12−14] Functionalization of the PAMAM branch ends with stearate groups makes these materials amphiphilic, and previous studies indicate that these polymers exhibit segregation when spread as monolayers at the air−water interface.[13,15] In this paper, we report the bulk phase behavior and microphase segregation of these semicrystalline PEO−PAMAM diblocks and their stearate-functionalized analogues in the solid state. These systems are the first such crystalline linear−dendritic block copolymers examined for bulk phase behavior. These materials, like those examined by Meier, are illustrative of the effect of the conformational asymmetry between the linear polymer chain and the highly branched dendron on block copolymer morphology. The crystallinity of the linear PEO block can greatly influence the final morphology; in these studies, observations of morphology were made above and below the crystalline melt point of PEO.

2. Experimental Section

The synthesis of the PEO−PAMAM diblocks has been described in detail in a separate paper;[12] the following is a brief summary description. Linear poly(ethylene oxide) was purchased from Shearwater polymers with a methoxy terminus and a primary amine terminus at either end of the linear chain (MW = 2000, PDI = 1.04). The dendrimer block was formed with the polyamidoamine (PAMAM) chemistry developed by Tomalia et al.[6] using the primary amine chain end as a reactive core for the buildup of the dendron. The first step in synthesizing the dendritic block is Michael addition of methyl acrylate. This is followed by amidation with ethylenediamine. The resulting PAMAM dendritic block is referred to as generation 1.0 and has two primary amine branch ends. Dendritic blocks of generations 1.0, 2.0, 3.0, and 4.0 with 2, 4, 8, and 16 branch ends have been synthesized by successively repeating the Michael addition and amidation reactions. ^{1}H NMR and FTIR spectra were determined after each reaction to confirm chemical structure and complete conversions. Molecular weight was determined by GPC as well as MALDI−TOFS.[12,14] Stearate functionalization of the primary amine branch ends of the dendron using stearic acid anhydride is described elsewhere.[13] The deuterated form of stearic acid was used because samples were also utilized for neutron reflectivity experiments in a separate publication.[15] Table 1 contains a summary of molecular weights and compositions for all samples. Molecular weights of the dendron block were determined based on the chemical structure presuming complete conversion at each generation, as verified by NMR.

Thin films for morphological characterization were solvent cast from chloroform at room temperature. First, 20 mg of polymer was dissolved in approximately 0.5 mL of chloroform, which is a good solvent for both PEO and PAMAM, and transferred dropwise onto a poly(tetrafluoroethylene) (Teflon) film placed inside a beaker vented to the atmosphere. Another open flask of chloroform was placed inside the beaker to slow the rate of solvent loss, allowing solvent annealing to attain films closer to their equilibrium state. After 4 days the cast films were transferred to a desiccator and stored for at least 1 week at room temperature prior to testing. For transmission electron microscopy (TEM) the films were cryotomed using an RMC ultramicrotome model MT-X with a diamond knife at −40 °C. Sections were transferred dry from the diamond knife surface onto copper grids and then stained with RuO_4 to provide contrast for electron imaging. TEM was performed on JEOL JEM 2000 FX and JEOL JEM 200 CX electron microscopes. Small-angle X-ray scattering (SAXS) experiments were done under vacuum using a Siemens computer-controlled system with a rotating anode producing Cu Kα radiation (λ = 1.54 Å) at 40 kV and 30 mA. Cast films for SAXS were enclosed in glass capillary tubes and placed in the hot stage. Additional X-ray data was collected on stearate-functionalized diblocks by moving the detector closer to the hot stage to access wider scattering angles.

Thermal characterization of both functionalized and unfunctionalized PEO−PAMAM diblocks was accomplished using differential scanning calorimetry (DSC)[12,14] and temperature-dependent SAXS. DSC scans were recorded on a Perkin-Elmer DSC7 calorimeter with heating and cooling rates of 10 °C/min. The amount of material used for the DSC runs was between 8 and 14 mg, and at least two scans were performed for each sample to eliminate any thermal history effects. X-ray experiments were conducted by placing the sample inside a hot stage placed in the beam path of the SAXS instrument. Data were collected at roughly 10 °C increments up to the thermal degradation point of the polymer. Wide-angle X-ray diffraction (WAXD) data were collected at various temperatures in the same fashion by repositioning the detector in the SAXS instrument to be closer to the sample. Temperature-dependent TEM studies were performed by heating samples in the SAXS hot stage and equilibrating at the desired temperature and then rapidly removing samples from the hot stage and quenching them in liquid nitrogen. After quenching, the samples were cryotomed and RuO_4 stained as described above.

3. Discussion

The chemical structure of a fourth generation linear−dendritic diblock, PEO(2000)−PAMAM generation 4.0, as well as a schematic cartoon of the polymer architecture, is shown in Figure 1a. The linear block is a monodisperse poly(ethylene oxide) (PEO) chain of molecular weight 2000, and the dendrimer block is a polyamidoamine (PAMAM) dendrimer. The amino end groups of the PAMAM block can also be functionalized with stearic acid to impart amphiphilic character, as illustrated in Figure 1b.

In previous work, we have described the behavior of PEO−PAMAM diblocks at the air−water interface[13,15] and in solution.[12] Pressure−area isotherms and neutron reflectivity experiments were used to characterize behavior at the air−water interface for PEO−PAMAM diblocks in which the dendrimer end groups were functionalized with stearic acid. These experiments showed that the stearate-functionalized diblocks were surface active and formed well-ordered monolayers with generation-dependent structure. The interfacial behavior of stearate functionalized PEO−PAMAM diblocks has shown the tendency of the blocks to segregate

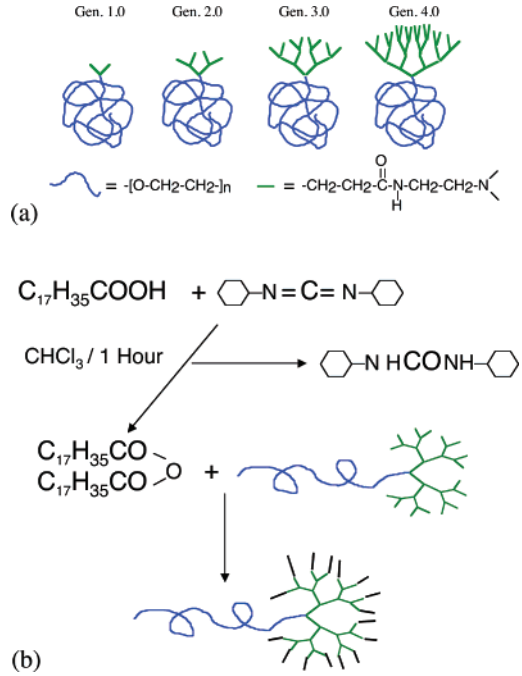

Figure 1. (a) Chemical structures of PEO(2000)−PAMAM generations 1.0−4.0 linear dendritic diblock copolymers. (b) Stearic acid functionalization of amino end groups of the PAMAM block.

within the overall monolayer structure.[15] Preliminary results from differential scanning calorimetry (DSC) and small-angle X-ray scattering (SAXS) indicate that PEO−PAMAM diblocks also exhibit microphase segregation in the bulk state.[13,14] These findings were of interest, particularly due to the relatively small size of the block copolymer systems, and their asymmetric architectures. In this paper, we seek to better understand the behavior of these materials in the bulk via morphological characterization using transmission electron microscopy (TEM) and SAXS. Thin films were prepared by solvent casting from $CHCl_3$ at room temperature onto a Teflon surface. For TEM the films were cryotomed with a diamond knife and stained with RuO_4 to provide contrast for electron images. The PAMAM block selectively absorbed RuO_4 during staining, as determined with stained controls of pure PEO homopolymer and PAMAM dendrimer homopolymer; the basis for staining is the binding of Ru to the carboxylamide groups in the PAMAM backbone. For SAXS experiments, the films were broken up and put into glass capillary tubes, which were then placed in a temperature controlled stage inside the SAXS instrument. Isothermal X-ray data were collected at a variety of temperatures up to the thermal degradation point of the polymer. Polymers were studied as a function of generation for both unfunctionalized amino terminated and stearate functionalized dendrons.

3.1. Unfunctionalized PEO−PAMAM Block Copolymers. Figure 2 contains a typical TEM image for PEO−PAMAM generation 1.0 formed at room temperature via slow evaporation of solvent. The dendrimer domains in this image appear as dark globules of approximately 20−30 Å, which form larger irregular aggregate clusters or superstructures of approximately 100−200 Å in diameter. PAMAM blocks from several molecules must aggregate together to form the smaller domains of 20−30 Å, as indicated by their size relative to the individual dendrons; the dendron size for generation 1.0 is about 7 Å. It is also possible at such small dimensions that the staining of the dendron block results in structures that appear somewhat larger than their actual size. Surrounding the aggregates is a continuous PEO-rich domain. Many isolated PAMAM dendrons are apparent as small dark gray spots of approximately 10 Å or less within the PEO-rich domain. It is clear that a good deal of phase mixing is evident in both the dendrimer aggregate and PEO rich domains, as indicated by the size of the features, the discontinuities within domains, and the presence of dendrons in the continuous domain; the larger aggregates appear to be clusters of dendritic domains, and light PEO regions are evident in these clusters. The tendency toward aggregation in dendritic polymers has been reported in other work;[18−21] in this case aggregation appears to take place in the block copolymer system, leading to a kind of larger scale segregation of the two blocks. This segregration is no doubt greatly influenced by the crystallization of the PEO block, and crystallinity is likely to be the driving force for phase segregation in such short block copolymer structure with a small dendritic block. The continuous phase appears to contain phase mixed copolymer, with the dendron blocks distributed evenly across the film. Temperature-dependent SAXS results in Figure 3 show a single peak at a *d* spacing of 140 Å that is observed from room temperature up to 70 °C. This *d* spacing agrees well with SAXS results for the crystalline PEO−NH_2 homopolymer starting material, and with published SAXS results for PEO of molecular weight 2000.[22−25] It is generally known that oligomers of PEO, much like those of polyethylene, will form unfolded, extended chain crystals at fairly low molecular weights; the extended length of an all-trans PEO chain of molecular weight 2000 is 140 Å, consistent with these observations.[22−25] This is particularly consistent with the highly regular, monodisperse PEO used for these studies (PDI = 1.04). DSC experiments on PEO−PAMAM generation 1.0 show that the PEO block melts at 52 °C.[14] A glass transition was not observed, nor were other endotherms observed in DSC. PEO−PAMAM generation 1.0 has a PAMAM volume fraction of about 3%, a weight fraction of 10%, and its morphology is dominated by the crystallinity of the PEO block. The PEO adopts the same

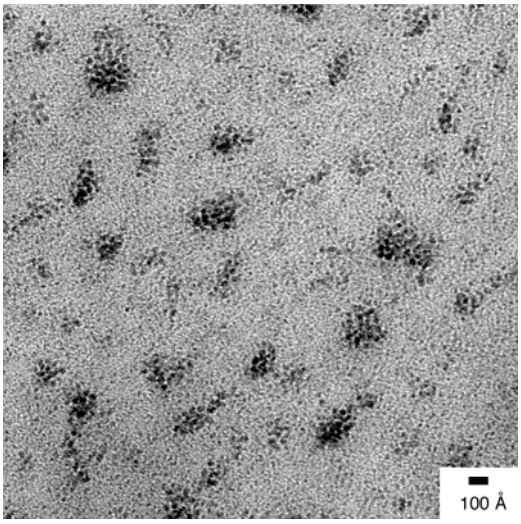

Figure 2. TEM image of PEO−PAMAM generation 1.0 bulk morphology at room temperature. All TEM images have PAMAM domains stained with ruthenium tetroxide.

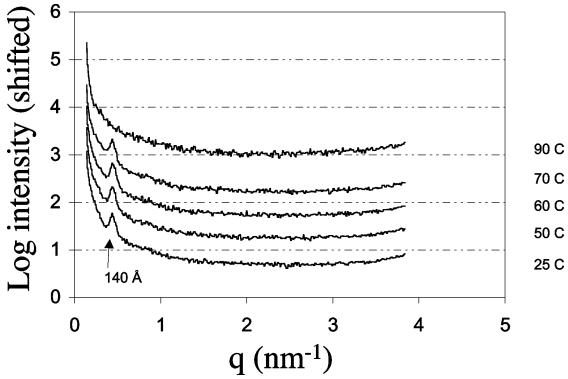

Figure 3. Temperature-dependent 1D SAXS profiles for PEO−PAMAM generation 1.0. Data are plotted as the log of relative scattered intensity log $I(q)$ vs the scattering vector q. All curves correspond to data collection for 1 h and have been shifted vertically to prevent overlap. The peaks are labeled with their d spacings.

crystalline form as the corresponding PEO homopolymer, but with the added constraint that chain ends with PAMAM dendrons tend to group together in roughly spherical aggregates. The result is an irregular disperse polymer morphology with a semicrystalline continuous matrix. The PEO crystallites exhibit a lowering of the melt transition due to the disruption of long-range order by the presence of the PAMAM blocks and aggregates of blocks. On close examination, the PEO crystalline lattice spacing of 4.5 Å can be seen in the TEM micrographs as swirling lines in the background. Upon melting of the PEO, the sample becomes fully phase mixed up to the thermal degradation point of the polymer. TEM micrographs of samples annealed above the T_m revealed little or no contrast. Differences between DSC and SAXS in the observed melting point of PEO are due to the differences in heat transfer for the two instruments.

3.2. Generation 2.0. There are four primary amine branch ends comprising the dendrimer block of PEO−PAMAM generation 2.0 and its PAMAM volume fraction is 8%. The dendron size for generation 2.0 is about 10 Å.[16,17,26] A typical TEM image of the morphology of the as-cast film (formed using a slow solvent evaporation process) exhibited by this polymer is shown in Figure 4a. The morphology is a weakly defined one that on close examination appears to consist of a continuous PEO domain containing small (diameter ∼20−30 Å) wormlike or rodlike domains of PAMAM. Figure 4b is a TEM of a sample with similar history; in this sample, some regions of the film exhibited morphologies that appear to be more ordered cylindrical phases. The crystallization of the PEO block prevents the attainment of highly ordered morphologies during the process of solvent evaporation; however, the image in Figure 4b appears to have been taken from a portion of the film for which the kinetics of crystallization were slow enough to allow a full attainment of the inherent diblock morphology. This anomaly may have been the result of fluctuations in air flow, temperature, etc., during sample preparation. These observations suggest that the native low temperature morphology of the diblock copolymer consists of weakly segregated cylinders or truncated cylinders. Both TEM images appear to exhibit a series of fine, faint lines indicative of the PEO crystalline lattice spacing of about 5 Å.

To examine the variation of morphology with temperature, temperature-dependent SAXS was performed.

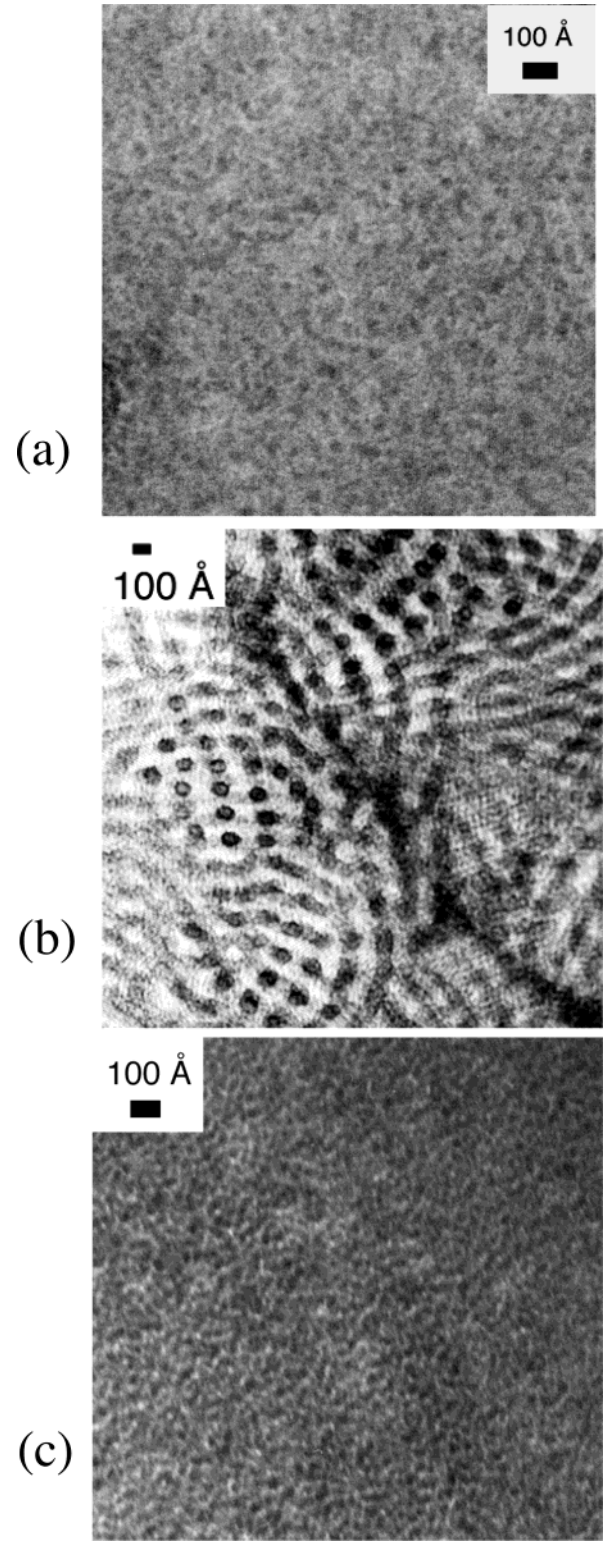

Figure 4. TEM images of PEO−PAMAM generation 2.0 bulk morphology: (a) room-temperature morphology; (b) room-temperature morphology associated with slower crystallization kinetics; (c) morphology of sample rapidly quenched from 75 °C.

The SAXS results for PEO−PAMAM generation 2.0 are shown in Figure 5; the 1-D profile at 25 °C contains a single peak at a d spacing of 37 Å. This peak is present from room temperature up to 60 °C, just beyond the PEO melting point, and appears to correspond roughly to the PEO crystalline spacing. Because of the presence of the larger generation 2.0 dendron as an end group

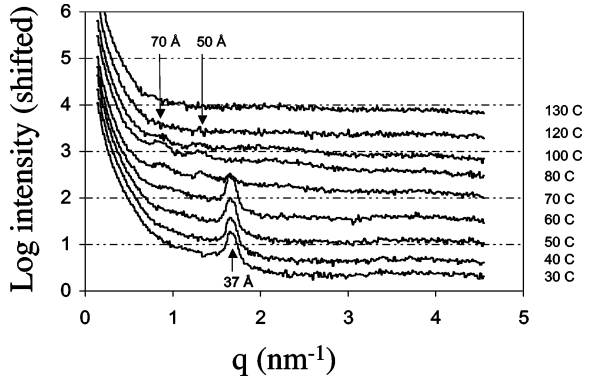

Figure 5. Temperature-dependent 1D SAXS profiles for PEO−PAMAM generation 2.0. Data are plotted as the log of relative scattered intensity log $I(q)$ vs the scattering vector q.

on the PEO, the packing of the oxyethylene chains in a crystalline lattice would be such that chain folding would be favored over extended chains. For this reason, it is likely that 37 Å indicates the PEO crystalline lamellar period. DSC results for PEO−PAMAM generation 2.0 show reversible PEO melting at 51 °C and the PAMAM glass transition at −20 °C. Again, differences in the temperatures at which transitions are observed in DSC and SAXS probably arise from the challenge of achieving heat transfer within the vacuum environment of the SAXS chamber. The changes observed in X-ray scattering at 60 °C are associated with the melting of these chain-folded PEO crystallites.[22−25] Just above the PEO melt point, there is still some order in the melt from 60 to 100 °C, as indicated by two faint peaks visible with SAXS at *d* spacings of 70 and 50 Å. The lower image in Figure 4c is from a sample quenched from 75 °C into liquid nitrogen in an attempt to capture the high temperature state of PEO−PAMAM generation 2.0. It shows closely spaced globular, wormlike PAMAM domains that are roughly 20 Å wide and 50−90 Å long. The lack of a regular ordered packing for these domains is consistent with the weak SAXS signal at this temperature; it is also possible that some of the order may have been destroyed upon quenching. The two SAXS *d* spacings at 50 and 70 Å appear to correspond to reflections from the morphology; the *d* spacing of 70 Å corresponds to an averaged period or spacing between domains, and the second peak may be a corresponding second-order reflection. The disappearance of thepeaks above 100 °C indicates the order−disorder transition of the polymer, following which it becomes completely phase mixed.

Above 60 °C, the constraint of the PEO crystallinity is removed, and the flexible PEO chains are able to take on statistical arrangements in space; the increased mobility of the polymer chains allow them to segregate into worm-shaped aggregates that resemble cylindrical morphologies. The suppression of block copolymer domain morphology by crystallinity was also reported by Register and co-workers for asymmetric semicrystalline−amorphous diblock copolymers consisting of polyethylene-*b*-poly(3-methyl-1-butene).[27,28] The degree of segregation between the blocks was found to affect the confinement of crystallization. For weakly segregated diblocks, crystallization completely disrupted the cylindrical morphology with slow cooling, while for strongly segregated diblocks, the confinement of crystallization inside cylinders was independent of thermal history. In this case, the segregation is weak, and therefore,

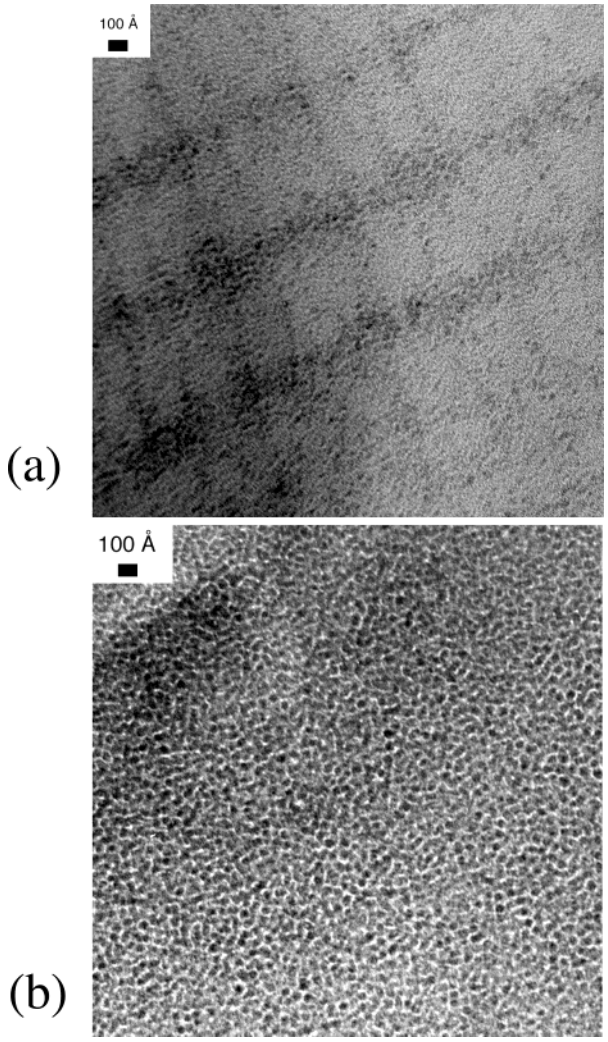

Figure 6. TEM images of PEO−PAMAM generation 4.0 bulk morphology: (a) room-temperature morphology; (b) high-temperature morphology from a sample rapidly quenched from 60 °C.

crystallinity remains relatively unconfined below the melt temperature. It is only in the slow-solvent annealed samples that block copolymer morphology is evident below the PEO melt temperature.

3.3. Higher Generation Unfunctionalized Systems. PEO−PAMAM generation 3.0 has a PAMAM volume fraction of 22% (weight fraction 45%) and generation 4.0 has a PAMAM volume fraction of 42% (weight fraction 63%). The dendron size is about 15 Å for generation 3.0 and about 20 Å for generation 4.0.[26] For these polymers, the dendron begins to approach the R_g of the linear block in its amorphous state. Parts a and b of Figure 6 contain the observed room temperature and high temperature morphology, respectively, of PEO−PAMAM generation 4.0. Both morphologies exhibit diffuse dark semicontinuous PAMAM rich domains within a continuous light PEO phase. The room-temperature morphology appears to contain a supermolecular scale order or superstructure that was observed in different samples. The gridlike spacings of clusters of PAMAM is believed to be an artifact of the solvent evaporation rate and the tendency of the dendritic domains to cluster and does not represent molecular scale order. Close inspection of the TEM reveals much smaller PAMAM domains within the lighter phase as well as the dark phase. The high-temperature morphol-

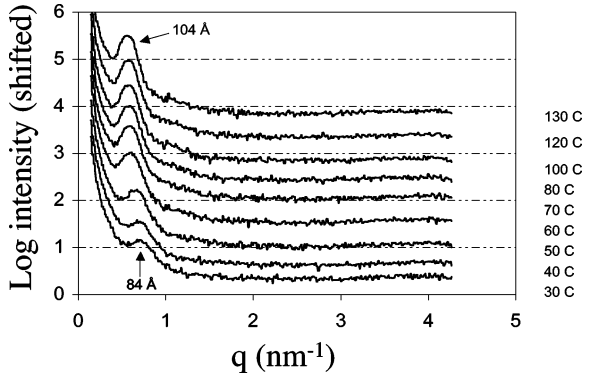

Figure 7. Temperature-dependent 1D SAXS profiles for PEO−PAMAM generation 4.0.

ogy, from a sample quenched into liquid nitrogen from 60 °C (above the PEO melt point), consists of wormlike PAMAM domains very similar to that observed for generation 2.0, but with a much denser concentration of stained PAMAM dendrons, resulting in a semicontinuous morphology. In this case, the domains are about 20 Å wide, close to the size of the generation 4.0 dendron. A bicontinuous morphology is actually what would be anticipated for an amorphous linear−dendritic diblock, based on the architectural asymmetry of the blocks, and the volume fraction of 43%.[11,29,30] TEM results for generation 3.0 showed distinct differences between high and low-temperature behavior, although no long-range order was observed at room temperature.

DSC thermographs taken of PEO−PAMAM generation 4.0 indicate the PAMAM glass transition to be 6 °C and the PEO melt transition is 40 °C. For generation 3.0 the T_g was found to be −11 °C and the T_m is 43 °C. These lowered T_g and T_m values indicate that some phase mixing is present in higher generation diblocks. SAXS results for generation 4.0, shown in Figure 7, indicate the presence of a single peak corresponding to a *d* spacing of 84 Å that persists up to 40 °C. Above 40 °C this peak shifts to a larger *d* spacing of 104 Å. The high-temperature *d* spacing of 104 Å corresponds to the predominant nearest-neighbor distance for the PAMAM domains. SAXS results for generation 3.0 show a high-temperature segregated melt state present above 50 °C, similar to generation 4.0. Below 50 °C, no SAXS peaks are observed, consistent with the room-temperature TEM for generation 3.0. In general, these observations are consistent with the soft confinement of PEO crystallinity reported by Zhu et al. for a lamellae-forming poly(ethylene oxide)-*b*-polystyrene diblock.[31] In this case, the diblock is blended with polystyrene homopolymer to alter the PEO crystallization temperature (T_c^{PEO}). When $T_{ODT} > T_c^{PEO} \geq T_g^{PS}$, heating the PEO crystals induces semicrystalline lamellar thickening, which ultimately destroys the block copolymer environment. Thickening was not observed for blends with hard confinement in which $T_{ODT} > T_g^{PS} > T_c^{PEO}$. The low PAMAM T_g definitely places PEO−PAMAM generation 3.0 and 4.0 in the soft confinement regime, making it possible for the PEO crystallinity to disrupt microphase segregation of the two blocks.

Alkyl-Terminated Dendritic Diblocks. The amino terminal groups at the ends of the dendritic branches in PEO−PAMAM were functionalized with stearate groups; this *n*-alkyl end-functionalization resulted in dendron blocks with a much more hydrophobic nature

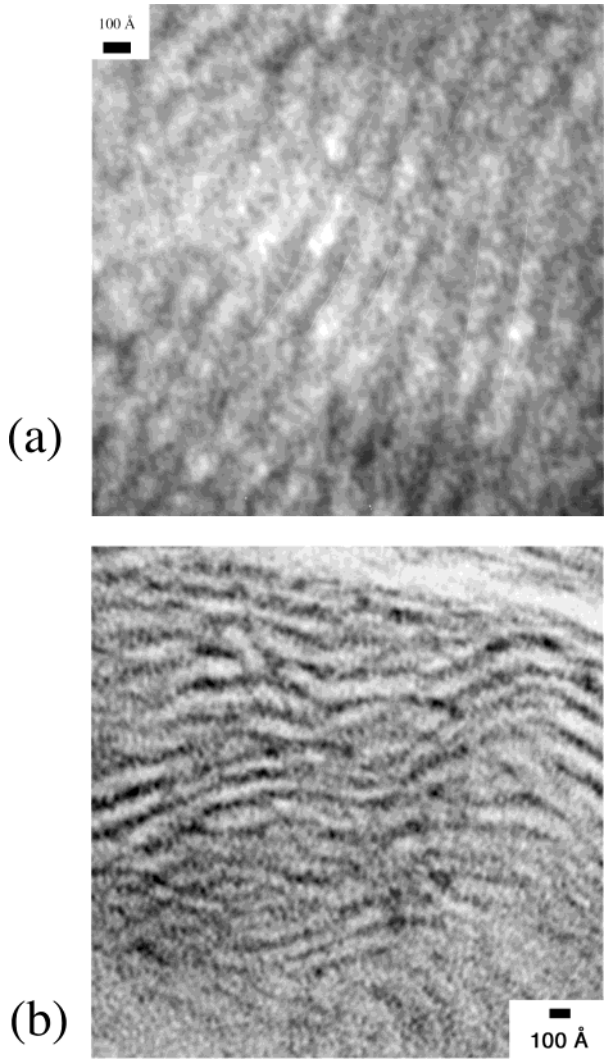

Figure 8. TEM image of PEO−PAMAM generation 1.0-S D_{35} bulk morphology: (a) room-temperature morphology, where white diagonal lines in the image represent damage to the photographic negative which occurred after the picture was taken; (b) morphology from sample annealed for 48 h at 40 °C.

than the original hydrophilic PAMAM, and end groups with a strong tendency toward ordering in the solid state. Because of the exponential number of end groups in the dendritic system, end functional groups can greatly influence the final properties of dendritic polymers, from surface properties to glass transition and ordering behavior. In this section, we examine the influence of the alkyl end groups as a means of directing the self-assembly of the block copolymers.

3.4. Generation 1.0-S D_{35}. Deuterated stearate modified PEO−PAMAM generation 1.0 (PEO−PAMAM 1.0-S) has a molecular weight of 2834, and the combined weight fraction of PAMAM plus stearate groups in the dendritic block is 29%. The size of the PAMAM dendron is about 7 Å, and the stearate groups have an extended chain length of about 18 Å. Figure 8a contains a TEM image of PEO−PAMAM 1.0-S in an as-cast film prepared using slow solvent evaporation from CHCl3; Figure 8b contains an example of the lamellar morphology which is more well-defined following annealing at 40 °C (below any observed melt points) for 48 h. In both cases, the lamellar periodicity is about 120 Å. SAXS results for PEO−PAMAM 1.0-S agree well with TEM,

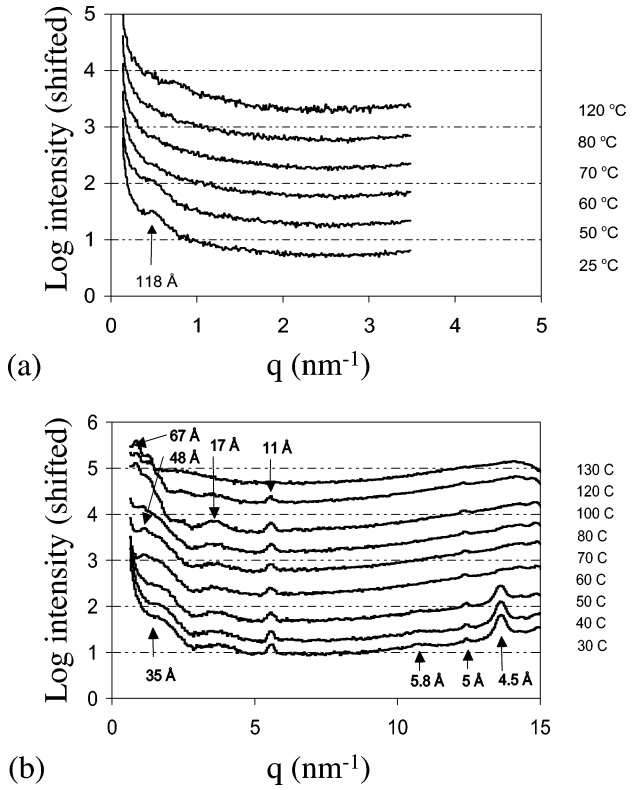

Figure 9. (a) Temperature-dependent 1D SAXS profiles for PEO−PAMAM generation 1.0-S D_{35}. (b) Temperature-dependent 1D WAXD profiles for PEO−PAMAM generation 1.0-S D_{35}.

as shown in Figure 9a; the diffractogram at room temperature contains a single broad peak corresponding to a *d* spacing of 118 Å. Thermal characterization of PEO−PAMAM 1.0-S with DSC revealed two endothermic transitions at 50 and 108 °C respectively, and no observable glass transitions above −20 °C. The SAXS diffractograms in Figure 9a indicate a disappearance of the SAXS peak between 50 and 60 °C, a temperature range that corresponds to the first of the endotherms observed in DSC. It is presumed that this first transition is the melt transition for the PEO block.

WAXD data were obtained as a function of temperature, as shown in Figure 9b, and indicate that both the PEO and the stearate groups are crystalline at room temperature. The crystalline PEO repeat units appear as a peak at $q = 14$ nm^{-1}, corresponding to a *d* spacing of 4.5 Å, and the crystalline stearate *d* spacings appear at 11, 17, and 35 Å (broad). The PEO and stearate crystalline peaks agree well with WAXD results for PEO homopolymer and stearic acid. The crystalline WAXD peak for PEO at 4.5 Å disappears completely at 60°C, consistent with the melt temperature of the PEO crystallites at 50−60 °C. Also at 60 °C, an additional broad peak appears at approximately 48 Å, and the 35 Å peak originally associated with the stearate groups becomes a shoulder to this new peak, resulting in a broad range of scattering at lower *q*. This new peak is probably indicative of a phase morphology corresponding to the amorphous PEO chains in the melt state, as opposed to the original crystalline state of the PEO, much as was observed in the nonfunctionalized PEO−PAMAM. The other WAXD peaks affiliated with stearate groups at *d* spacings of 17, 11, and 5 Å are visible up to 120 °C, well above the melt point of stearic acid of 71 °C; there is apparent order in the melt state of the block copolymer. The 35 Å shoulder also disappears at this temperature, resulting in a narrowing of the broad peak at low *q*. The disappearance of these peaks agrees well with the second DSC endothermic transition at 108 °C and corresponds to the isotropization of a high-temperature mesophase exhibited by the diblock copolymer above the PEO melt point. The presence of multiple endotherms and order in the melt state is consistent with liquid crystalline ordered phases. In this case, the presence of the alkyl chains appears to induce thermotropic ordering in the melt state; mesophase order is known to exist in alkyl-terminated molecular systems, ranging from traditional surfactant molecules to alkyl-terminated smectic liquid crystals and main chain and side chain polymers, due to the strong tendency of the alkyl systems to pack effectively. Above the 108 °C clearing point (determined in DSC), the WAXD peaks associated with stearate groups become less intense and disappear completely at 130 °C, leaving only the broad, ill-defined peaks at 67 Å and 48 Å. These broad peaks, which appear to exist between 60 and 130 °C, are likely to correspond to reflections of weakly segregated block copolymer domains in the absence of crystalline or liquid crystalline order.

From the above observations, it is clear that the introduction of long alkyl chains as dendritic end groups greatly affects the room-temperature morphology, resulting in a clear lamellar morphology instead of the disperse disordered globular PAMAM domains and aggregates observed for the unfunctionalized sample in Figure 2. This difference is due to the strong tendency of alkyl chains to pack into ordered layered structures. It is also notable that the stearate chains also significantly altered the phase behavior of these systems. The unfunctionalized PEO−PAMAM 1.0 only exhibits a single melt point, beyond which the system is completely disordered—there is no crystalline or block copolymer phase order remaining. For the alkyl-functionalized system, there is a crystalline PEO melt point and a long-lived thermotropic liquid crystalline phase that persists out to 120 °C before complete clearing. It is not apparent from these studies whether a weak form of phase segregated order might exist beyond this temperature; although SAXS does not yield evidence of any well-ordered morphological structure, structure is observed in WAXD at low *q*.

3.5. Generation 2.0-S D_{35}. PEO−PAMAM 2.0-S has four deuterated stearate groups attached to the PAMAM branch ends for a total molecular weight of 3890; the combined weight fraction of PAMAM and stearate groups in this case is 49%. Figure 10a contains representative TEM images of PEO−PAMAM generation 2.0-S lamellar morphologies formed from slow solvent evaporation at room temperature. This clear lamellar morphology has a periodicity in these samples of approximately 40 Å based on TEM. From previous DSC analysis, three well-defined endotherms are observed at 39, 118, and 146 °C. No glass transitions were observed for this polymer above −20 °C.

X-ray scattering results shown in Figure 11 give some insight into the ordering and phase changes taking place as a function of temperature in this system. SAXS data (Figure 11a) indicate that at room temperature, a peak at a *d* spacing of 37 Å is present that corresponds well to the observed TEM micrographs for the room-temperature sample. A second peak at 33 Å corresponds well to a characteristic spacing in stearate ordering. This stearate ordering peak was not observed in SAXS data

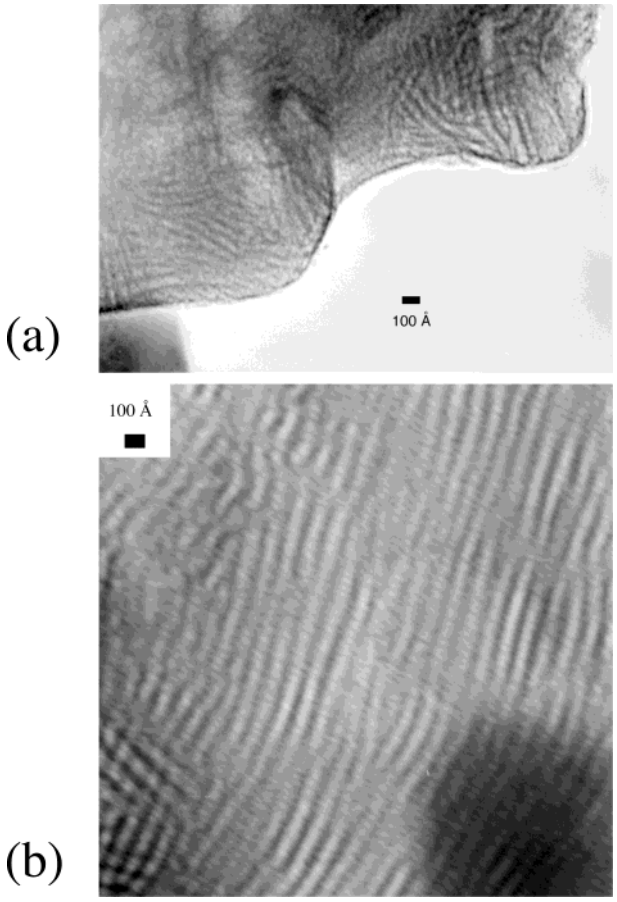

Figure 10. TEM images of PEO−PAMAM generation 2.0-S D35 bulk morphology: (a) image of room-temperature morphology; (b) image taken from sample rapidly quenched from 120 °C.

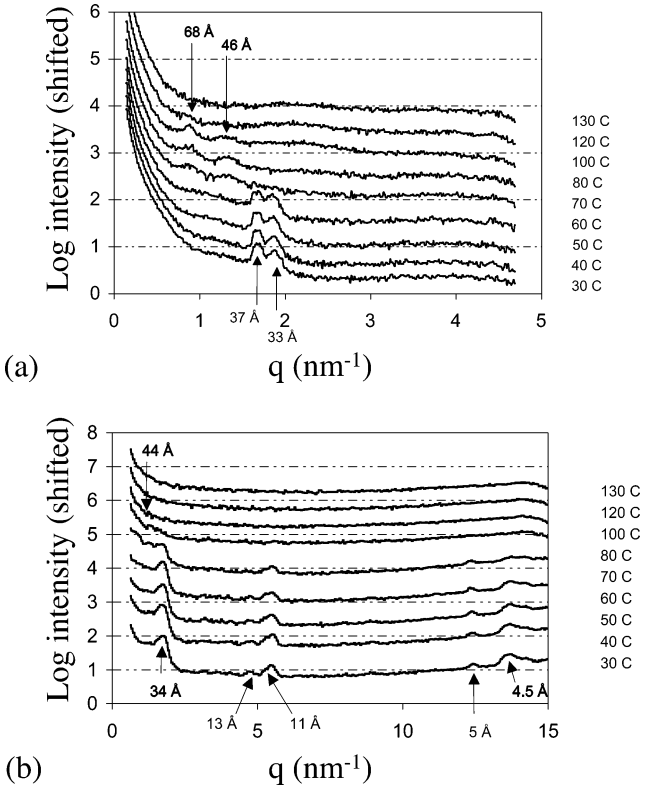

Figure 11. (a) Temperature-dependent 1D SAXS profiles for PEO−PAMAM generation 2.0-S D_{35}. (b) Temperature-dependent 1D WAXD profiles for PEO−PAMAM generation 2.0-S D_{35}.

for PEO−PAMAM 1.0-S because the volume fraction of stearate groups was too low for ordering to take place. SAXS peaks for generation 2.0-S are present up to the PEO melt point at 60 °C, above which they abruptly disappear; this transition corresponds roughly to the endotherm observed at 40°. Differences in heat transfer and flux within the two different hot stages, particularly with a difference in a vacuum vs atmospheric conditions may account for some discrepancies in observed temperature; furthermore, the endotherms observed in DSC were quite broad, and generally exhibited a 20 °C bandwidth. Above 60 °C, two new, much broader peaks appear at *d* spacings of 68 and 46 Å that persist up to 120 °C, where the peaks are greatly diminished. These *d* spacings are very similar to those observed at higher temperatures in WAXD data for the generation 1.0 diblock and appear to correspond to the endotherm obtained in DSC at 118 °C. It is believed that the phases that exist above the PEO melting point are thermotropic mesophases, as described for PEO−PAMAM 1.0-S. Temperature-dependent WAXD results for PEO−PAMAM 2.0-S, shown in Figure 11b, confirms that the crystalline PEO (*d* spacing 4.5 Å) melts at 60 °C, and the stearate groups (*d* spacing 34, 13, 11, 4.1 Å) undergo some disordering at approximately 80 °C. The high-temperature SAXS peaks at 46 and 68 Å (and the WAXD peak at 44 Å) indicate that the PEO−PAMAM 2.0-S exhibits a segregated block copolymer melt state at high temperatures, similar to those observed in unfunctionalized PEO−PAMAM. The lower image in Figure 10b is taken from a sample quenched from 120 °C with liquid nitrogen. The lamellar periodicity in this case is still quite pronounced, and appears to represent the mesophase between 60 and 120 °C, which re-forms rapidly during the quench experiment. It is interesting to note that the *d* spacing observed in this sample is 100−110 Å, higher than the originally observed spacing of 40 Å. This new spacing is much higher than the highest visible SAXS peak *d* spacing of 68 Å, suggesting the possibility that a first-order reflection for the lamellar morphology may be missing. If the two small broad peaks visible in SAXS at this temperature range are presumed to be second and third order reflections, of a lamellar morphology, the first-order reflection would be approximately 136 Å. Finally, there is a third reversible DSC endotherm at 130°C; because long time annealing at temperatures much higher than 120 °C can lead to degradation of the PAMAM dendron, it was not possible to discern the order at such high temperatures. The lack of diffraction in both small and wide-angle X-ray suggests that if order is present, it is weak, and the dendron contains no positional order (e.g., akin to a high-temperature nematic phase).

The morphological state of PEO−PAMAM generation 2.0-S appears to be lamellar both above and below the PEO melting point. This is consistent with the concept of strong confinement of the PEO crystallinity by the block copolymer morphology, such that the lamellar morphology is preserved during the transition from the melt state to room temperature. The addition of the hydrocarbon stearate groups to the PAMAM branch ends in this case may serve to promote the strong segregation case for confined crystallization described by Quiram and co-workers, via a mechanism of increased interaction parameter (lowered compatibility between blocks).[27,28] It is also possible that the mesophase ordered state of the stearate groups, as seen with

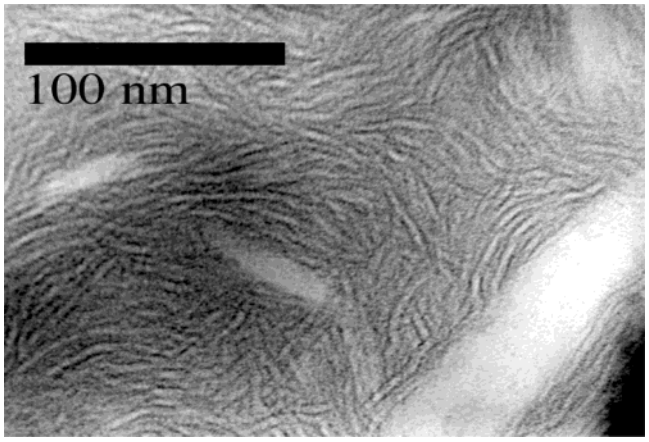

Figure 12. TEM image of PEO−PAMAM generation 3.0-S D_{35} bulk morphology at room temperature.

WAXD, results in a kind of hard confinement of the PEO crystallization as described by Zhu et al.; where in this case $T_{ODT} > T_{lc}^{sterate} > T_c^{PEO}$.[31] In this scenario, stearate groups would tend to ensure segregation between the blocks at high temperatures where the PEO block has melted and is no longer discernible with WAXD or SAXS.

3.6. Higher Generation Stearate-Functionalized Systems. Generations 3 and 4 exhibited morphological phase behavior very similar to that of PEO−PAMAM-2.0-S; both exhibit lamellar morphologies and multiple DSC endotherms associated with the loss of crystallinity and disordering of the stearate chains. PEO−PAMAM-3.0-S has a molecular weight of 6035 and a combined weight fraction of PAMAM and stearate groups of 67%, whereas PEO−PAMAM-4.0-S has a molecular weight of 10252, with 16 stearate groups attached to its dendron branch ends, and a combined weight fraction of PAMAM and stearate groups of 80%.

The ordering behavior observed with temperature in WAXD and SAXS was very similar for generations 3 and 4. The TEM for PEO−PAMAM-3.0-S is shown in Figure 12, and the TEM and SAXS results for PEO−PAMAM-4.0-S are shown in Figures 13 and 14, respectively. Despite the high weight fraction of 80% functionalized dendrimer in PEO−PAMAM-4.0-S, the morphology of this system remains lamellar (see Figure 13), as do all the lower generations of stearate functionalized diblocks. TEM images of this system are very similar to those observed for generation 3.0-S, although the micrographs indicated slightly less well-defined domains. Similarly, the generation 1.0 block copolymer also exhibited less apparent order based on TEM. This phenomenon may be due, in part, to the fact that at the more asymmetric compositions, it is more difficult to induce well-defined lamellar ordering. For PEO−PAMAM-4.0-S, the lamellar periodicity at room temperature is about 85 Å, and DSC data indicate three endotherms at 37, 60, and 100 °C. Lamellar periodicity for generation 3.0-S was found to be 70 Å (TEM) and DSC indicates endotherms at 32, 65, and 110 °C.

Temperature-dependent diffraction studies are shown in Figure 14a (SAXS) and 13b (WAXD). First and second-order reflections at 94 Å (weak shoulder) and 47 Å in SAXS due to the lamellar block morphology are visible, though weak, at low temperature. Above 60°C, these morphology peaks shift, and the higher order peak completely disappears, resulting in a *d* spacing at 60 Å. This peak, in turn, disappears at 120−130 °C,

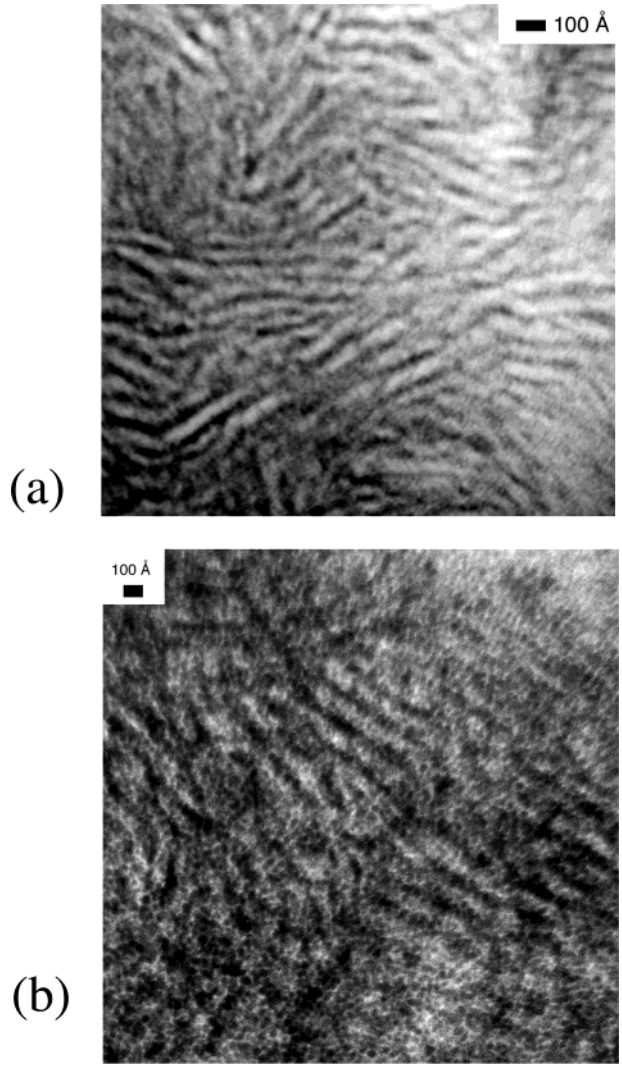

Figure 13. (a, b) TEM images of PEO−PAMAM generation 4.0-S D_{35} bulk morphology at room temperature.

leaving a very weak and ill-defined diffraction peak at 130 °C corresponding to 30 Å, which may be affiliated with residual order in the block copolymer melt prior to the ODT. WAXD and SAXS provide evidence of the loss of PEO crystalline order at 60 °C (*d* spacings at 4.5 Å) and confirm the transition in stearate ordering via loss of peaks at 38, 33, 19, 13, and 7.7 Å at 70 °C. Remaining order persists in the mesophase up to 100−120 °C as indicated by the persistence of the peak at 11 Å, corresponding to the highest temperature endotherm observed in DSC; at this point, the stearate-induced LC order clears. Between 120 and 130 °C there is also a single broad peak visible in WAXD at a *d* spacing of 32 Å, consistent with the broad reflection seen in SAXS; these findings suggest that, on the disappearance of the stearate mesophase ordering, the block copolymer appears to undergo an order−order transition (an OOT as opposed to an ODT), possibly to a highly disordered, weakly segregrated morphology at 130°C.

Temperature-dependent SAXS results for generation 3.0-S (not shown) indicate the presence of peaks at low temperature at *d* spacings of 38 and 36 Å, corresponding to the stearate group packing, present below 70 °C. There are also broad peaks at *d* spacings of 92 and 45 Å that correspond to the first and second-order reflections from the lamellar morphology observed with TEM.

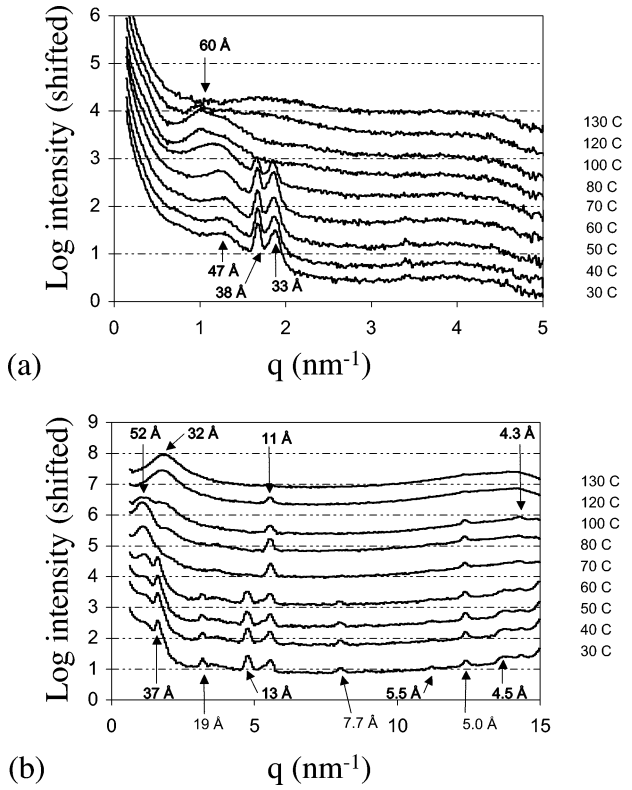

Figure 14. (a) Temperature-dependent 1D SAXS profiles for PEO−PAMAM generation 4.0-S D_{35}. (b) Temperature-dependent 1D WAXD profiles for PEO−PAMAM generation 4.0-S D_{35}.

In general, observations of multiple endotherms and ordered melt states are consistent for generations 1.0−4.0. This information suggests that the alkyl chains undergo an order−order or LC transition at 60−70 °C typical of crystal−smectic phase transitions in liquid crystalline thermotropic mesophases. At 110−120 °C, a second ordering transition takes place, resulting in a loss of the higher order mesophase behavior, and an absence of peaks in WAXD and SAXS. It is apparent that both the phase segregated morphological order seen at higher *d* spacings (lower *q*) and the smectic ordering disappear simultaneously at this temperature. In studies of side chain LC−amorphous block copolymers, we have observed similar LC isotropization induced block copolymer order−disorder transitions (ODT's);[32,33] it is likely that similar behavior occurs in this case. Birefringence was observed for the alkyl functional diblocks in polarizing optical microscopy at temperatures above 60°C, confirming the presence of an ordered mesophase above the melt point.

Perhaps even more remarkable is the fact that, despite the broad range of weight fractions examined, from approximately 70% linear PEO to as low as 20% PEO, the morphology remained lamellar for the stearate functionalized systems, whereas the unfunctionalized systems exhibited a variation in morphologies observed in solvent cast films, including disperse and cylindrical morphologies. A schematic summarizing a model of the behavior of the stearate-functionalized dendritic systems as observed with DSC, X-ray diffraction, and TEM, is shown in Figure 15.

Slowly evaporated solvent cast films or films annealed at low temperatures exhibited lamellar morphologies; however, WAXD and SAXS verified the presence of PEO crystallinity, as well as crystalline or a highly ordered state for the alkyl end groups. The fully extended form

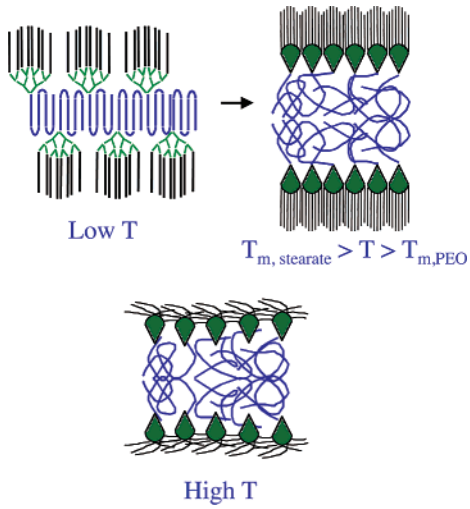

Figure 15. Schematic illustrations of high- and low-temperature morphology for stearate-functionalized PEO−PAMAM.

of PEO was observed in PEO−PAMAM 1.0-S, as indicated by a broad peak in SAXS at 118 Å at temperatures below the PEO melt point; however, at higher generations, the PEO crystallites appear to take on smaller dimensions based on SAXS that are indicative of chain folded PEO lamellae. It is reasonable to anticipate chain folding as the size of the dendrimer increases, as was observed for the unfunctionalized species, due to space filling requirements. The dendritic block is pushed out of the crystalline regions, forming separate segregated domains containing the PAMAM branched structure. Finally, the stearate end groups form what is essentially a third phase, with a high degree of order. Based on WAXD, the stearate groups take on ordering similar to their crystalline form in stearic acid, with all-trans, fully extended conformations. It is likely that at low temperatures, these stearate groups may order at a given tilt angle with respect to the lamellar plane. The PAMAM dendrimer portion may be relatively compressed within the proposed lamellar structure; Langmuir−Blodgett studies of PAMAM homopolymers functionalized with alkyl groups indicate that the alkyl chains all orient at the surface, spreading and compressing the dendrimer at the air−water interface.[34] On heating, the PEO crystallites melt, thus introducing mobility to the block copolymer structure. The result is an ordered melt; shortly above the PEO melt, the stearate groups appear to undergo an order−order phase change characteristic of a crystal-to-smectic or smectic-to-smectic transition, as evidenced by the presence of an endotherm in DSC, and the loss of some peaks in DSC, but the persistence of other WAXD peaks to high temperatures. Finally, at very high temperatures, the stearate chains lose all of their organization. In the cases of the higher generations, phase segregation is relatively strong, and the block copolymer morphology is stable to relatively high temperatures.

Some trends can be observed in going from low to high generation number in the stearate-functionalized systems. The generation 1.0, consisting of only two stearate end groups, exhibits a lamellar spacing close to that of chain extended PEO, and its morphology can be described as that of an extended chain crystal containing ordered alkyl end groups. If one considers the possibility of tilt of the PEO chains, and the stearate chains, with respect to the plane of the lamellae, it is possible to allow

for the size of the alkyl chains and the 120 Å extended PEO chains. Further, it is highly likely that the PEO chains interpenetrate upon assembly. By taking into account both considerations, it is possible to have a PEO crystalline lamellar region within the block copolymer of less than 120 Å thickness. This first generation species is the only one of the stearate-functionalized series to exhibit only two endotherms. On heating this crystalline block copolymer beyond the PEO melting point, the alkyl chains remain ordered, allowing the formation of a liquid mesophase which persists to 120 °C. Generation 2.0 and all higher generations exhibit strong peaks in SAXS at 37 to 33 Å, which disappear at the PEO melting point, and appear to be related to a folded chain crystalline form of PEO; there is no sign of the original chain extended PEO form at 25 °C in any of the three higher generations. On the other hand, when the generation 2.0 system undergoes the ordering transition at the PEO melt point, it exhibits the peaks at 68 and 46 Å, in positions similar to those seen in generation 1.0 at higher temperature. If, once again, these are taken to represent second and third-order reflections, the corresponding *d* spacing would be 136 Å. It is possible that generation 2.0 orders in a manner similar to generation 1.0 at high temperature, with fully extended chains in an ordered mesophase, and stearates ordered about the crystalline lamellae; however, at low temperature, its behavior is much more like that of generations 3 and 4. These last two higher generation polymers also undergo multiple phase transitions in the DSC. The lowest temperature endotherms probably correspond to polymorphic ordering changes below the PEO melting point, or the melting of highly unstable, small crystallites. In both generations, the lamellar block copolymer structure is clearly indentifiable at room temperature, when the PEO is in its crystalline state; the block copolymer morphology is manifest by SAXS peaks at approximately 85 and 90 Å respectively. Above the PEO melt point, these morphologies exhibit single peaks at intermediate spacings of 60 to 65 Å. In this case, as illustrated in the schematic, the PEO block is assumed to take on a random coil arrangement in the LC phase as well as the isotropic melt, and the alkyl chains are the primary ordered entity in the mesophase up to 120 to 130 °C. Beyond these temperatures, some weak phase segregation may still exist; however, it was not detected in these samples with WAXD or SAXS.

4. Conclusions

TEM, SAXS, and DSC have been used to characterize microphase segregation in the bulk state for PEO−PAMAM linear−dendritic diblock copolymers. The linear block for these materials consisted of 2000 molecular weight monodisperse poly(ethylene oxide) (PEO) and the dendrimer block was a polyamidoamine (PAMAM) dendron. The primary amine branch ends of the PAMAM block were functionalized with stearic acid to impart amphiphilic character to the diblocks. Both functionalized and unfunctionalized diblocks of generations 1.0 through 4.0 were solvent cast into thin films for morphology characterization. All samples except the unfunctionalized generation 1.0 exhibited a segregated melt state at temperatures above the melting point of the PEO block. For the unfunctionalized diblocks generations 2.0 through 4.0 showed PAMAM domains in the melt shaped like elongated globules or worms. The stearate-functionalized diblocks showed a segregated melt state in at high temperatures for generations 1.0−4.0 and a high-temperature lamellar morphology was observed with TEM for generation 2.0-S. At lower temperatures the PEO block underwent confined crystallization. The extent of confinement varied with PAMAM generation and end group functionalization. For the unfunctionalized diblocks, the PAMAM T_g was below room-temperature such that there was soft confinement of the PEO crystallinity. Soft confinement resulted in the complete disruption of morphology for the unfunctionalized generation 3.0 and generations 2.0 and 4.0 exhibited room-temperature morphologies that differed from the melt state. For the functionalized diblocks, the attached stearate groups crystallized at or above the PEO melting point so that there was hard confinement of the PEO crystallinity. This prevented the PEO from disrupting the PAMAM-rich domains, and lamellar morphology was observed at room temperature for all generations of functionalized diblocks.

Acknowledgment. The authors acknowledge the Environmental Protection Agency for funding under Grant No. R825224-01-0. We are also grateful to A. Moment of MIT for assistance with cryotoming PEO−PAMAM and M. Frongillo of the MIT CMSE for help with TEM.

References and Notes

(1) Jansen, J. F. G. A.; de Brabaamder-van den Berg, E. M. M.; Meijer, E. W. *Science* **1994**, *266*, 1226−1229.
(2) Balogh, L.; Tomalia, D. A. *J. Am. Chem. Soc.* **1998**, *120*, 7355−7356.
(3) Esumi, K.; Suzuki, A.; Yamahira, A.; Torigoe, K. *Langmuir* **2000**, *16*, 2604−2608.
(4) Gröhn, F.; Kim, G.; Bauer, B. J.; Amis, E. J. *Macromolecules* **2001**, *34*, 2179−2185.
(5) Zhao, M.; Sun, L.; Crooks, R. M. *J. Am. Chem. Soc.* **1998**, *120*, 4877−4878.
(6) Tomalia, D. A. N.; Goddard, W. A. *Angew. Chem., Int. Ed. Engl.* **1990**, *29*, 9, 138−175.
(7) Gitsov, I.; Wooley, K. L.; Fréchet, J. M. J. *Angew. Chem., Int. Ed. Engl.* **1992**, *31*, 1200−1202.
(8) Gitsov, I.; Wooley, K. L.; Fréchet, J. M. J. *J. Am. Chem. Soc.* **1996**, *118*, 3785−3786.
(9) Yu, D.; Vladimirov, N.; Fréchet, J. M. J. *Macromolecules* **1999**, *32*, 5186−5192.
(10) Gitsov, I.; Wooley, K. L.; Hawker, C. J.; Ivanova, P. T.; Fréchet, J. M. J. *Macromolecules* **1993**, *26*, 5621−5627.
(11) Roman, C.; Fischer, H. R.; Meijer, E. W. *Macromolecules* **1999**, *32*, 5525−5531.
(12) Iyer, J.; Hammond, P. T. *Macromolecules* **1998**, *31*, 8757−8765.
(13) Iyer, J.; Hammond, P. T. *Langmuir* **1999**, *15*, 1299−1306.
(14) Iyer, J. Doctoral Dissertation. Chemical Engineering Department, Massachusetts Institute of Technology, Cambridge, MA, 1999.
(15) Johnson, M. A.; Santini, C. M. B.; Iyer, J.; Satija, S.; Ivkov, R.; Hammond, P. T. *Macromolecules* **2002**, *35*, 231−238.
(16) Bauer, B. J.; Topp, A.; Prosa, T. J.; Amis, E. J.; Yin, R.; Qin, D.; Tomalia, D. A. *Abstr. Pap. Am. Chem. Soc.* **1997**, *214*.
(17) Stechemesser, S.; Eimer, W. *Macromolecules* **1997**, *30*, 2204−2206.
(18) Aoi, K.; Motoda, A.; Okada, M. *Macromol. Rapid Commun.* **1997**, *18*, 945−952.
(19) Chapman, T. M.; Hillyer, G. L.; Mahan, E. J.; Shaffer, K. A. *J. Am. Chem. Soc.* **1994**, *116*, 11195.
(20) van Hest, J. C. M.; Baars, M. W. P. L.; Elissen-Roman, C.; van Genderen, M. H. P.; Meijer, E. W. *Macromolecules* **1995**, *28*, 6689−6691.
(21) van Hest, J. C. M.; Delnoye, D. A. P.; Baars, M. W. P. L.; van Genderen, M. H. P.; Meier, E. W. *Science* **1995**, *268*, 1592−1595.

(22) Cheng, S. Z. D.; Chen, J.; Herberer, D. P. *Polymer* **1992**, *33*, 1429−1436.
(23) Cheng, S. Z. D.; Wu, S. S.; Chen, J.; Zhuo, Q.; Quirk, R. P.; von Meerwall, E. D.; Hsiao, B. S.; Habenschuss, A.; Zschack, P. R. *Macromolecules* **1993**, *26*, 5105−5117.
(24) Kovacs, A. J.; Gonthier, A. *Colloid Polym. Sci.* **1972**, *250*, 530−551.
(25) Kovacs, A. J.; Gonthier, A.; Straupe, C. *J. Polym. Sci., Polym. Symp.* **1975**, *50*, 283−325.
(26) Tomalia, D. A. B.; V.; Hall, M.; Hedstrand, D. M. *Macromolecules* **1987**, *20*, 1164.
(27) Quiram, D. J.; Register, R. A.; Marchland, G. R. *Macromolecules* **1997**, *30*, 4551−4558.
(28) Quiram, D. J.; Register, R. A.; Marchland, G. R.; Ryan, A. J. *Macromolecules* **1997**, *30*, 8338−8343.
(29) Johnson, M. A. Doctoral Dissertation. Chemical Engineering Department, Massachusetts Institute of Technology, Cambridge, MA, 2002.
(30) Anthamatten, M. L.; Hammond, P. T. *J. Polym. Sci., Part B: Polym. Phys.* **2001**, *39*, 2671−2691.
(31) Zhu, L.; Mimnaugh, B. R.; Qing, G.; Quirk, R. P.; Cheng, S. Z. D.; Thomas, E. L.; Lotz, B.; Hsiao, B. S.; Yeh, F.; Liu, L. *Polymer* **2001**, *42*, 9121−9131.
(32) Anthamatten, M. L.; Zheng, W. Y.; Hammond, P. T. *Macromolecules* **1999**, *32*, 4838−4848.
(33) Zeng, F.; Zimmerman, S. C. *Chem. Rev.* **1997**, *97*, 1681−1712.
(34) Nierengarten, J. F.; Eckert, J. F.; Rio, Y.; Carreon, M. D. P.; Gallani, J. L.; Guillon, D. *J. Am. Chem. Soc.* **2001**, *123*, 9743−9748.
(35) Mackay, M. E.; Hong, Y.; Jeong, M.; Tande, B. M.; Wagner, N. J.; Hong, S.; Gido, S. P.; Vestberg, R.; Hawker, C. J. *Macromolecules* **2002**, *35*, 8391−8399.
(36) Pochan, D. J.; Pakstis, L.; Huang, E.; Hawker, C. J.; Pople, J. *Macromolecules*, **2002**, *35*, 9239−9242.

MA030450M